NASA Technical Memorandum 106248
ICOMP–93–21

Numerical Simulations of Three-Dimensional Laminar Flow Over a Backward Facing Step; Flow Near Side Walls

Erlendur Steinthorsson
Institute for Computational Mechanics in Propulsion
Lewis Research Center
Cleveland, Ohio

Meng-Sing Liou and Louis A. Povinelli
Lewis Research Center
Cleveland, Ohio

and

Andrea Arnone
Institute for Computational Mechanics in Propulsion
Lewis Research Center
Cleveland, Ohio

Prepared for the
1993 ASME Fluids Engineering Division Conference
Symposium on Separated Flows
Washington, D.C., June 20–24, 1993

NASA

ICOMP
Lewis Research Center
Ohio Aerospace Institute
INSTITUTE FOR COMPUTATIONAL MECHANICS IN PROPULSION

NUMERICAL SIMULATIONS OF THREE-DIMENSIONAL LAMINAR FLOW OVER A BACKWARD FACING STEP; FLOW NEAR SIDE WALLS

Erlendur Steinthorsson
Institute for Computational Mechanics in Propulsion
Lewis Research Center
Cleveland, Ohio 44135

Meng-Sing Liou and Louis A. Povinelli
National Aeronautics and Space Administration
Lewis Research Center
Cleveland, Ohio 44135

Andrea Arnone
Institute for Computational Mechanics in Propulsion
Lewis Research Center
Cleveland, Ohio 44135
and Department of Energy Engineering
University of Florence
Florence, Italy

ABSTRACT

This paper reports the results of numerical simulations of steady, laminar flow over a backward-facing step. The governing equations used in the simulations are the full "compressible" Navier-Stokes equations, solutions to which were computed by using a cell-centered, finite volume discretization. The convection terms of the governing equations were approximated with an accurate, hybrid flux-vector splitting/flux-difference splitting scheme (second order upwind differencing). The validity and accuracy of the numerical solutions were verified by comparing the results to existing experimental data for flow at identical Reynolds numbers in the same backstep geometry. The paper focuses attention on the details of the flow field near the side wall of the geometry.

INTRODUCTION

As a frequently used model of separated flows, flow over a backward-facing step (backstep flow) can be considered a fundamental or prototype flow in fluid mechanics which should be thoroughly investigated until a complete understanding of the flow is achieved. Accordingly, a large number of investigations of backstep flows have been reported over the years, both experimental and theoretical (numerical). Most experimental investigations of backstep flows have focused on turbulent flows. These investigations have examined different aspects of backstep flows, such as heat-transfer characteristics downstream of the step (e.g., Vogel and Eaton, 1985), the effect of turbulence intensity on the reattachment process (e.g., Isomoto and Honami, 1989), and transient behavior of backstep flows (e.g., Tsou, *et al.*, 1991). One of the latest reported experimental studies was done by Hasan (1992) who examined modes of instability in the shear layer after a laminar separation. One of relatively few investigations of laminar backstep flows was reported by Armaly, *et al.* (1983) who studied backstep flows over a range of Reynolds numbers from laminar to fully turbulent flow. They reported spanwise measurements of velocity profiles and reattachment lengths in addition to measurements in the center plane of the channel. These measurements showed that, except in the immediate neighborhood of sidewalls, the flow is two dimensional for Reynolds numbers in the lower end of the laminar range as well as for Reynolds numbers in the turbulent range. At intermediate Reynolds numbers the flow was found to be three-dimensional over the entire width of the channel. The vast majority of experimental studies have examined flows at Reynolds numbers in the two-dimensional range with measurements taken in the center region of the channel.

Just as the nature and objectives of experimental studies have varied widely, so have the nature and objectives of numerical studies. Most numerical studies reported to date have been two-dimensional and, like the experimental studies, have focused on turbulent flows. In recent years, a number of three-dimensional studies have been reported. Several of these studies were large eddy simulations undertaken to examine the structure of the turbulent flow field (Schmitt and Friedrich, 1987; Arnal and Friedrich, 1991; Silveira, *et al.*, 1991). Three-dimensional studies have also been undertaken to examine instability waves and transition to turbulence (e.g., Kaiktsis, et al. 1991). Some of the reported numerical studies, both two- and three-dimensional, had as their primary objective to validate numerical codes (e.g., Ku, *et al.*, 1989) or to test and compare the performance of turbulence models in separated flows (e.g., Thangam and Hur, 1991; Thangam and Speziale, 1992). Like the experimental investigations, few numerical investigations have paid significant attention to the flow field near the sidewalls of the backstep geometries.

The purpose of this paper is to report a three-dimensional numerical study of the flow field near the sidewalls in laminar backstep flows. The geometry chosen for this study is

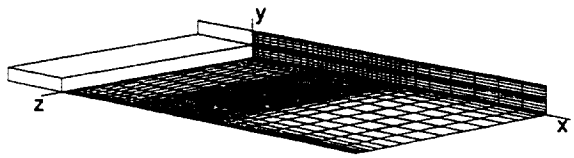

Figure 1. Backward-facing step geometry and grid system (only every fourth grid line is plotted in the x- and y-coordinate directions).

the same as the one used by Armaly *et al.* (1983) in their experimental work. Velocity profiles and reattachment lengths obtained in this study are compared to those measured by Armaly and coworkers in order to verify the validity of the present computations. The paper is organized as follows: At the completion of this introduction, the methodology employed in this study is described. Afterwards, results of simulations for three different Reynolds numbers are presented and flow patterns in the neighborhood of the sidewalls are shown and discussed. The paper concludes with a short summary.

METHODOLOGY

The governing equations used in this study are the "compressible" Navier–Stokes equations; i.e., the continuity equation, momentum equations and the total-energy equation (see e.g., Schlichting, 1979). Since the Mach number of flow to be modelled is low, the fluid is assumed to be a thermally and calorically perfect gas with dynamic viscosity that is a linear function of temperature.

Numerical solutions to the governing equations were obtained by using a modified version of a computer code called TRAF3D (transonic-flow-3D; Arnone, et al., 1991 and 1992). TRAF3D employs a cell-centered, finite-volume spatial discretization of the governing equations. In the modified version of TRAF3D, the convection terms of the governing equations are approximated by using second-order accurate upwind differencing in conjunction with the advection upwind splitting method (AUSM)—a recently developed upwind differencing scheme for the compressible Navier-Stokes equations (Liou and Steffen, 1991). The AUSM scheme is a hybrid flux-vector-splitting (FVS) / flux-difference-splitting (FDS) scheme (Corier and van Leer, 1991). It has the simplicity of FVS schemes while its accuracy has been shown to rival or exceed that of the best FDS schemes (Liou and Steffen, 1991). Diffusion terms are approximated by using standard second-order accurate difference formulas. TRAF3D uses a four-stage Runge-Kutta time-stepping scheme to integrate the governing equations in time (Jameson, *et al.*, 1981). Convergence to steady state is accelerated by using a multi-grid technique in conjunction with local time-stepping and implicit residual smoothing. For a detailed description of the numerical method of solution see Arnone, *et al.* (1991)

In the computations of the backstep flows reported in this paper, four types of boundary conditions were employed. At the inlet, the incoming Riemann invariant was specified

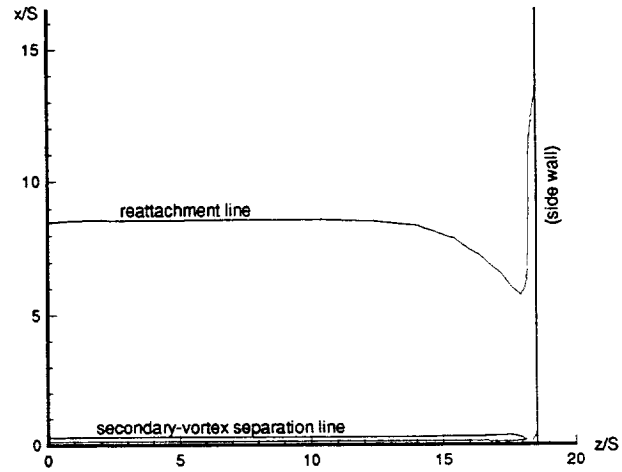

Figure 2. Reattachment line for the primary vortex, and separation line for the secondary vortex on the channel floor ($Re = 389$).

corresponding to a flow of uniform static pressure and temperature and a parabolic velocity profile. To mimic the sidewall boundary layer of the incoming flow, the velocity was gradually reduced to zero at the sidewall using a cubic profile and a specified boundary layer thickness. The maximum velocity of the incoming flow was taken to correspond to a local Mach number of 0.1. At the outflow boundary, a constant back-pressure was prescribed whereas density and velocity were extrapolated. On solid walls, no-slip adiabatic wall conditions were applied. Finally, symmetry conditions were applied at the center of the channel since computations were performed for only one half of the channel.

RESULTS

Results were obtained for the backward-facing step geometry shown in the sketch of Fig. 1. The geometry has an expansion ratio $H/h = 1.94$, where h is the channel height up-stream of the step and H is the channel height downstream of the step, and an aspect ratio $W/S = 37.1$, where W is the width of the channel and S is the step height. This geometry is the same as the one used by Armaly, *et al.* (1983).

The grid system used in all computations is also shown in Fig. 1. The figure shows the grid lines in the symmetry plane of the channel ($z = 0$) and on the channel floor ($y = 0$). Note, only every fourth grid line is plotted. The grid system employed for the three-dimensional simulation contained 65 grid points from the floor of the channel to the ceiling, 161 grid points from the step to the outflow boundary located 30 step-heights from the step, and 25 grid points from the symmetry plane of the channel to the sidewall. Two-dimensional computations were done on a grid consisting of a single 161×65 plane. As Fig. 1 shows, grid points were clustered near all solid surfaces and midway between the channel floor and the channel ceiling.

Numerical simulations of the flow in the backward facing step geometry shown in Fig. 1 were computed for Reynolds

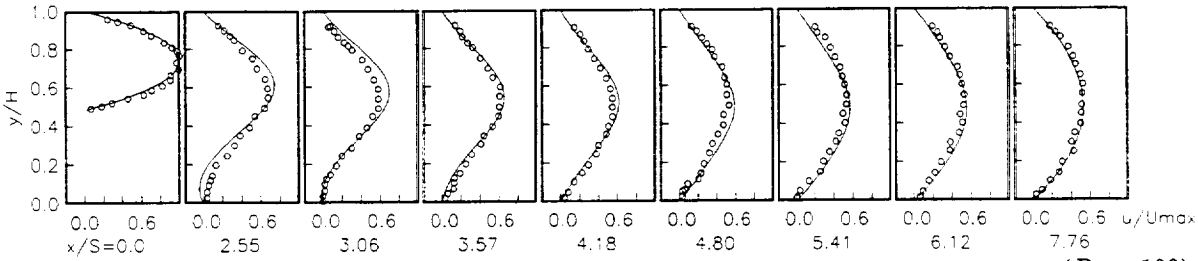

Figure 3. Velocity profiles in symmetry plane of backward-facing step geometry ($Re = 100$).
o Armaly, *et al.* (1983) — two-dimensional simulation.

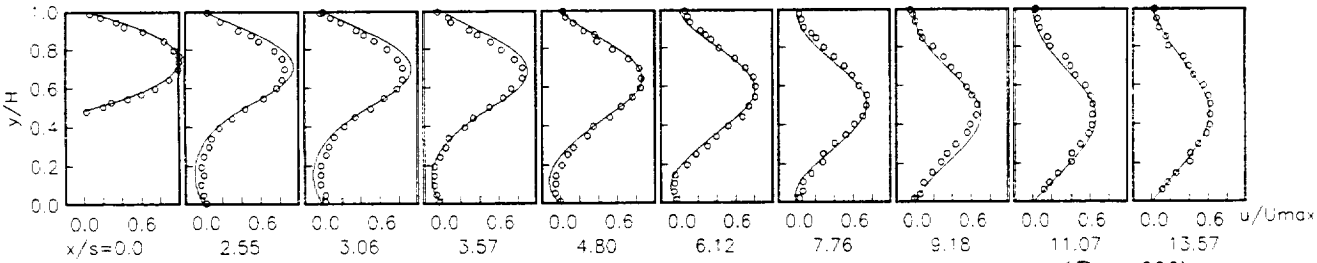

Figure 4. Velocity profiles in symmetry plane of backward-facing step geometry ($Re = 389$).
o Armaly, *et al.* (1983) — two-dimensional simulation.

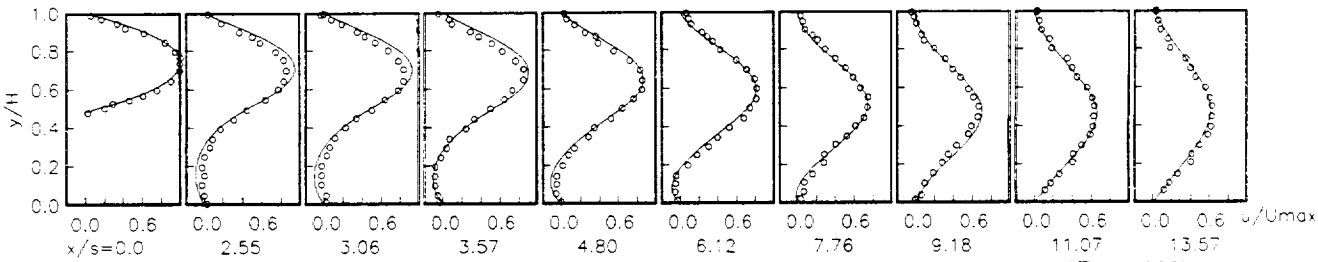

Figure 5. Velocity profiles in symmetry plane of backward-facing step geometry ($Re = 389$).
o Armaly, *et al.* (1983) — three-dimensional simulation.

numbers of 100 and 389 ($Re = U_{max}D/\nu$, where U_{max} and ν, respectively, are the flow-speed and kinematic viscosity of the incoming flow, and $D = 2h$ is the hydraulic diameter of the upstream channel). Two-dimensional simulations were done for $Re = 100$, but both two- and three-dimensional simulations were done for $Re = 389$.

The quality of the numerical results can be evaluated by comparing computed reattachment lengths and velocity profiles to the measured quantities reported by Armaly, *et al.*, (1983) for the same backstep geometry. The measured reattachment location for $Re = 100$ was reported to be at approximately $x/S = 3.3$ and at approximately $x/S = 8$ for $Re = 389$. In the experiments, the flow was essentially two-dimensional at both these Reynolds numbers. The predicted reattachment length based on the two-dimensional computations for $Re = 100$ was right on target, at $x/S = 3.3$, whereas for $Re = 389$ the computed reattachment length was slightly overpredicted, at $x/S = 8.7$—around 10% error. The three-dimensional computations for $Re = 389$ did somewhat better, predicting the reattachment at $x/S = 8.5$. Figure 2 shows the predicted spanwise variation in reattachment length for $Re = 389$. The figure shows that the reattachment length is constant over most of the span but starts decreasing approximately five step-heights away from the sidewall at $z/S = 18.55$. The reattachment length reaches a minimum of $5.73S$ at $z/S = 17.95$, where it starts to increase rapidly (the reasons for this behavior will be examined later). In the experiments, however, the reattachment length was constant at least up to 2.5 step-heights away from the wall (measurements were not taken closer to the wall than this). This difference between the predicted and measured behavior could be the result of a too thick incoming sidewall boundary-layer being used in the computations. No information was given in Armaly, *et al.* (1983) about the thickness of the incoming boundary layer. Here, a thickness corresponding to 3% of the channel width was used.

Figures 3 to 5 show a comparison of predicted and measured profiles of x-component of velocity in the symmetry plane of the channel. Figure 3 shows the velocity profiles for $Re = 100$, whereas Fig. 4 and 5 show the velocity profiles for $Re = 389$ based on the two- and three-dimensional computations, respectively. The velocity profiles obtained in the three-dimensional simulation for $Re = 389$ are almost iden-

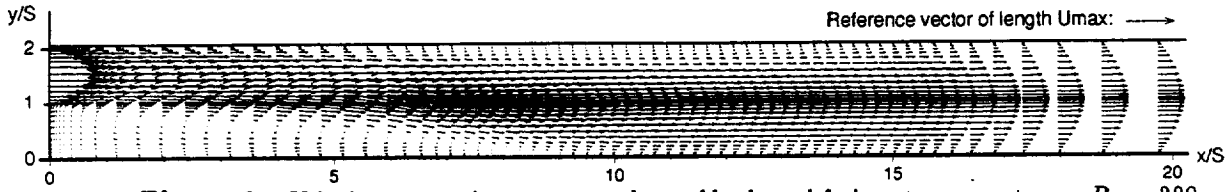

Figure 6. Velocity vectors in symmetry plane of backward-facing step geometry — $Re = 389$; three-dimensional simulation.

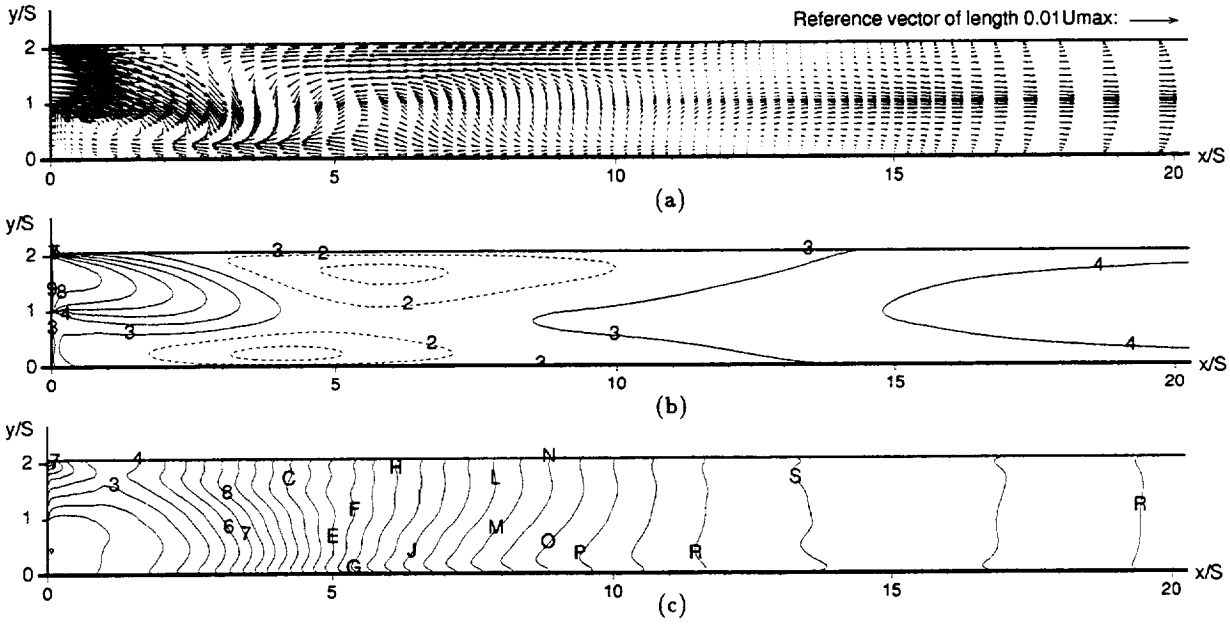

Figure 7. Flow near sidewall of backward-facing step geometry — $Re = 389$; three-dimensional simulation. (a) Velocity vectors. (b) Contours of u/U_{max}: $(u/U_{max})_1 = -0.004$, $\Delta(u/U_{max}) = 0.002$. (c) Contours of normalized pressure: $R_1 = 0.99915$, $\Delta P = 0.00005$.

tical to those obtained in the two-dimensional simulation. Although some overshoot in the magnitude of the velocity can be seen in all the simulations for both Reynolds numbers, the computed and measured velocity profiles compare very well with all inflection points in the velocity profiles properly predicted. Overall, the quality of the numerical results is good.

Figures 6 and 7 show the flow conditions in two, constant-z, cross-sections of the channel. Figure 6 shows a plot of the velocity vectors in the symmetry plane of the channel. The figure shows clearly the main recirculation zone behind the step. Although it cannot be seen in this figure, a secondary recirculation zone was obtained in the corner between the step and the channel floor. This secondary recirculation region is responsible for the separation line plotted in Fig. 2. Figures 7a to 7c show the velocity vectors, contours of x-component of velocity (u), and pressure contours in a plane located 0.005 step-heights away from the side wall. Note, the length of the vectors in Fig. 7a has been magnified hundredfold compared to that in Fig. 6, and that the broken contours in Fig. 7b correspond to negative values of the velocity component. Figures 7a and 7b reveal a large region of reversed flow in the immediate neighborhood of the sidewall. The presence of this recirculation region can be attributed to the pressure rise that occurs in the channel as the incoming flow expands and slows down. The low-momentum fluid in the sidewall boundary layer of the incoming flow cannot overcome this pressure gradient and the flow separates. Downstream of the main reattachment location (at $x/S = 8.5$) the flow gradually recovers. As Fig. 7b shows, the flow recovers first midway between the channel floor and the channel ceiling and recovers last near the floor and ceiling. The reason for this behavior is the interplay between the pressure gradient in the channel and the viscous forces acting on the fluid. On one hand, as Fig. 7c shows, there is an adverse pressure gradient up to about $x/S = 14$, with the pressure gradient being steepest between $x/S = 3$ and $x/S = 7$. On the other hand, the velocity in the core of the channel is highest midway between the floor and ceiling of the channel, causing relatively high sheer stresses near the wall. Consequently, midway between the floor and the ceiling the flow is able to overcome the pressure gradient as early as at $x/S = 8.5$. However, closer to the floor and the ceiling of the channel, the sheer stresses are lower so the flow recovers later. In the corners between the sidewall on one hand and the floor or the ceiling on the other, the flow

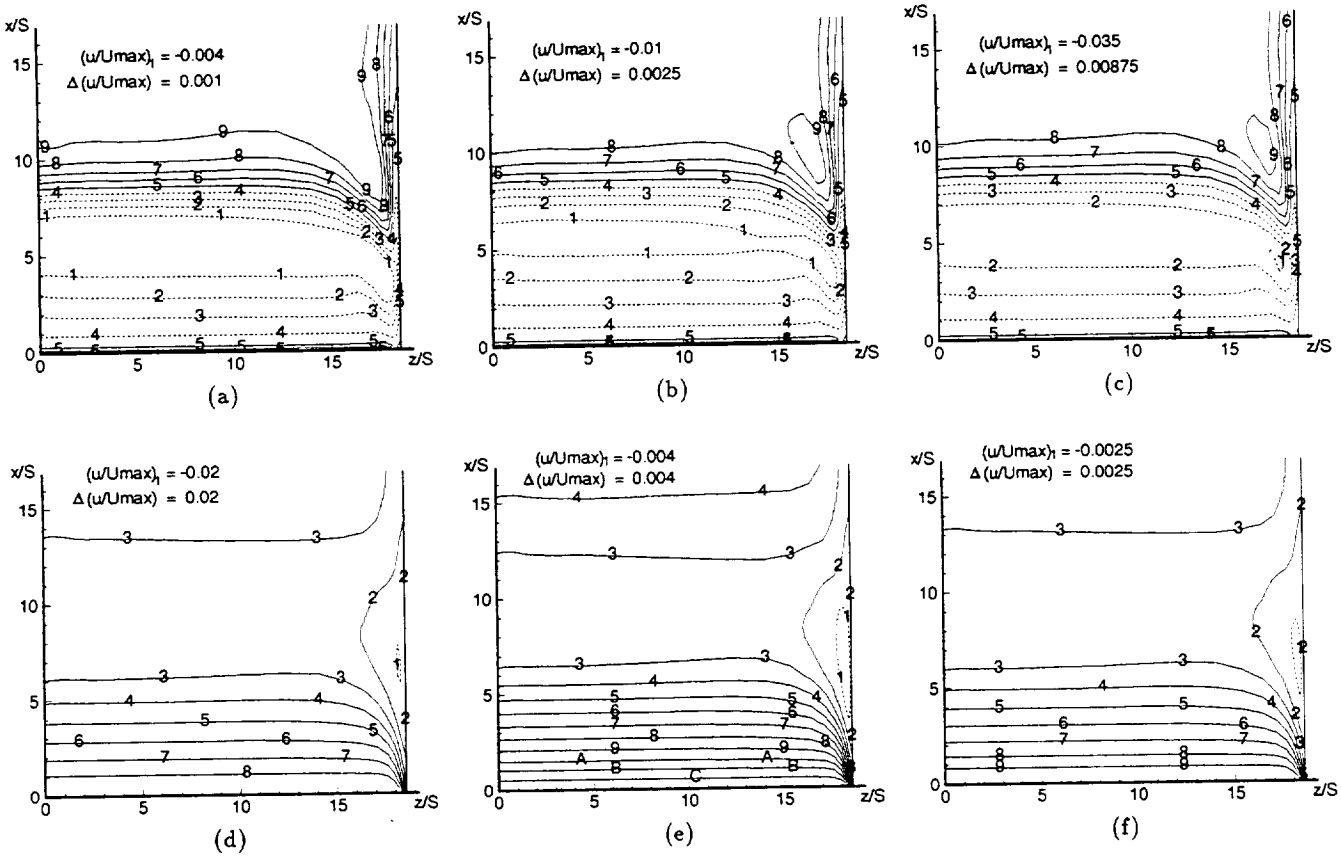

Figure 8. Contours of u/U_{max} in constant-y cross-sections — $Re = 389$; three-dimensional simulation. (a) $y/S = 0.005$, (b) $y/S = 0.011$, (c) $y/S = 0.038$, (d) $y/S = 2.023$, (e) $y/S = 2.050$, (f) $y/S = 2.056$.

cannot withstand any pressure gradient so the flow is reversed as long as there is an adverse pressure gradient in the channel.

With the above discussion in mind we can now explain the shape of the reattachment line in Fig. 2. In the main part of the channel (i.e., between $z/S = 0$ and $z/S = 13.5$), the flow is essentially two dimensional which results in constant reattachment length. Closer to the sidewall, momentum of the incoming fluid is lower than in the main part due to the sidewall boundary layer. This causes the reattachment length to degrease, as seen in Fig. 2. However, very close to the wall the adverse pressure gradient in the channel is the primary driving force in fluid, causing reversed flow as long as the adverse pressure gradient persists. This causes an increase in the reattachment length very close to the wall. At $z/S = 17.95$, the effects of decreasing momentum of the incoming flow and the effects of the adverse pressure gradient are in balance that corresponds to the minimum reattachment length.

Figure 8 shows contours of the x-component of velocity in constant-y cross-sections at various distances above the channel floor. Figures 8a–8c show the velocity contours near the channel floor, whereas Fig. 8d–8f show the contours near the ceiling. As before, the broken contour lines correspond to negative values of the velocity component. These figures show the spanwise variation in the velocity and the shape of the region of reversed flow that was revealed in Fig. 7. Figures 8a–8c show that a region of positive velocity exists adjacent to the step. This region is due to the secondary recirculation zone in the corner between the step and the channel floor. Figures 8d–8f show clearly the separation bubble that is created at the sidewall due to the adverse pressure gradient in the channel.

Figure 9 shows contours of the x-component of velocity near the sidewall in cross-sections at several streamwise locations. Figure 8a shows that the incoming boundary layer on the side wall starts to separate in the corner between the sidewall and the ceiling of the channel. This separation region grows in the streamwise direction and at approximately $x/S = 4$. (Fig. 9b) the entire boundary layer has detached. The strength of the reversed flow continues to increase in the upper corner until around $x/S = 7$. (Fig. 9d) but decreases after that. In the lower corner the reversed flow is strongest at approximately $x/S = 4$. (Fig. 9b) but decreases in strength after that as the main flow in the channel reattaches to the channel floor. After $x/S = 12$. (Fig. 9f) the reversed flow persists only in the upper and lower corners.

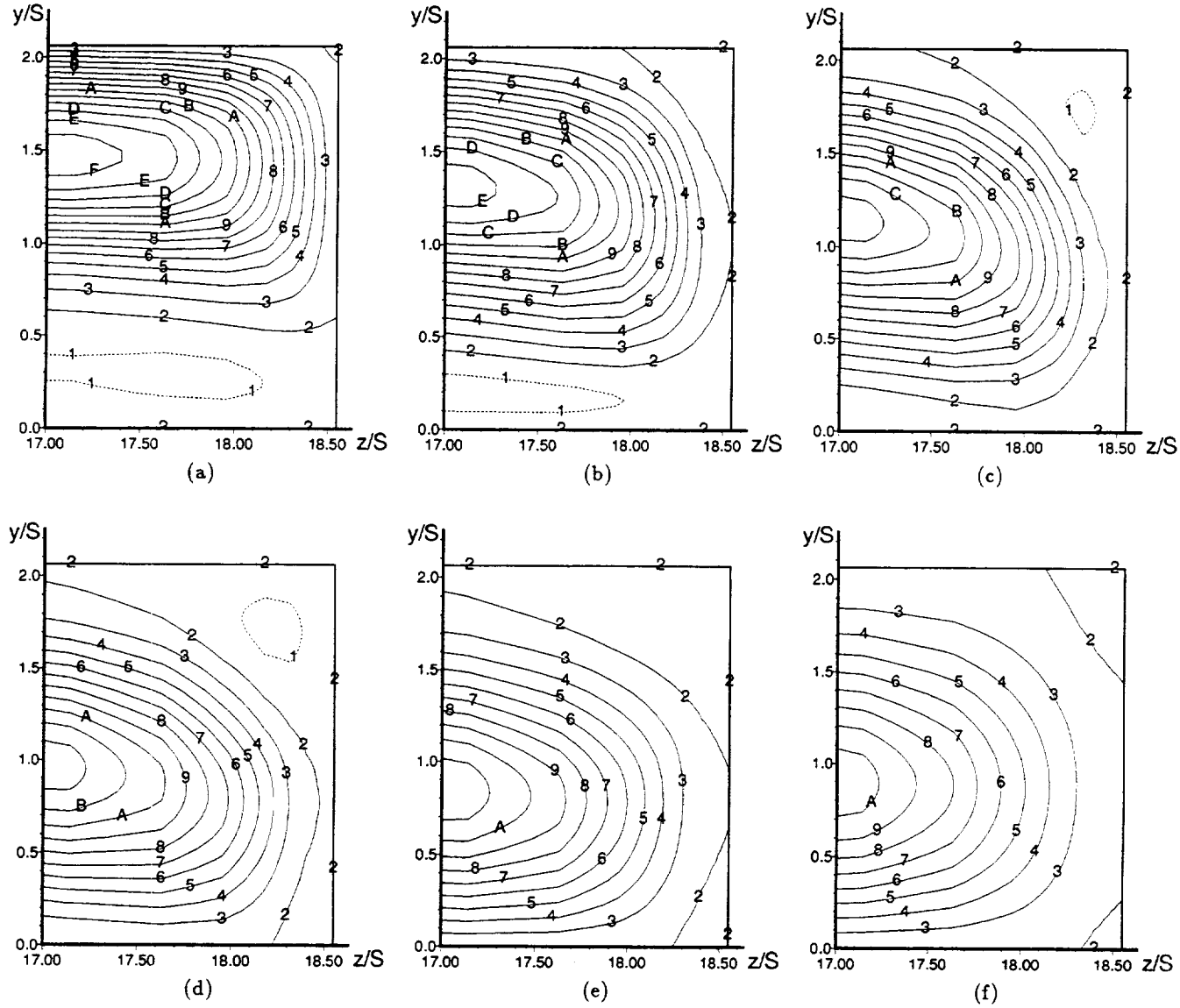

Figure 9. Contours of u/U_{max} in constant-x cross-sections — $Re = 389$; three-dimensional simulation. $(u/U_{max})_1 = -0.004$, $\Delta(u/U_{max}) = 0.002$.
(a) $x/S = 1.98$, (b) $x/S = 3.98$, (c) $x/S = 5.38$, (d) $x/S = 6.96$, (e) $x/S = 9.00$, (f) $x/S = 12.00$.

Finally, Fig. 10 and 11 show cross-flow velocity vectors near the sidewall at several streamwise locations. These figures reveal the existence of strong cross flow and streamwise vortices in the corner between the sidewall and channel floor. Figure 10b shows clearly the counter-clockwise rotating vortex in the lower corner. The size of this vortex grows in the streamwise direction as is seen in Fig. 10c to 10e. Figure 11a shows an enlarged view of the lower corner region in Fig. 10c. This figure shows that the counter-clockwise rotating vortex observed in Fig. 10b-10f gives rise to a weaker clockwise rotating vortex deeper in the corner. Fig. 11b and 11c show that this vortex persists further downstream. The strength of the recirculation diminishes after $x/S = 9$.

SUMMARY

A numerical investigation of three-dimensional laminar flow over a backward-facing step has been carried out. The investigation focused on the the flow field near the sidewalls of the backstep geometry. The investigation revealed a complicated flow pattern near the sidewall. This complicated flow pattern was created by interplay between the effects of the main recirculation region behind the step, the adverse pressure gradient that is created when the incoming flow expands and slows down, and the low-momentum fluid in the incoming boundary layer on the sidewall.

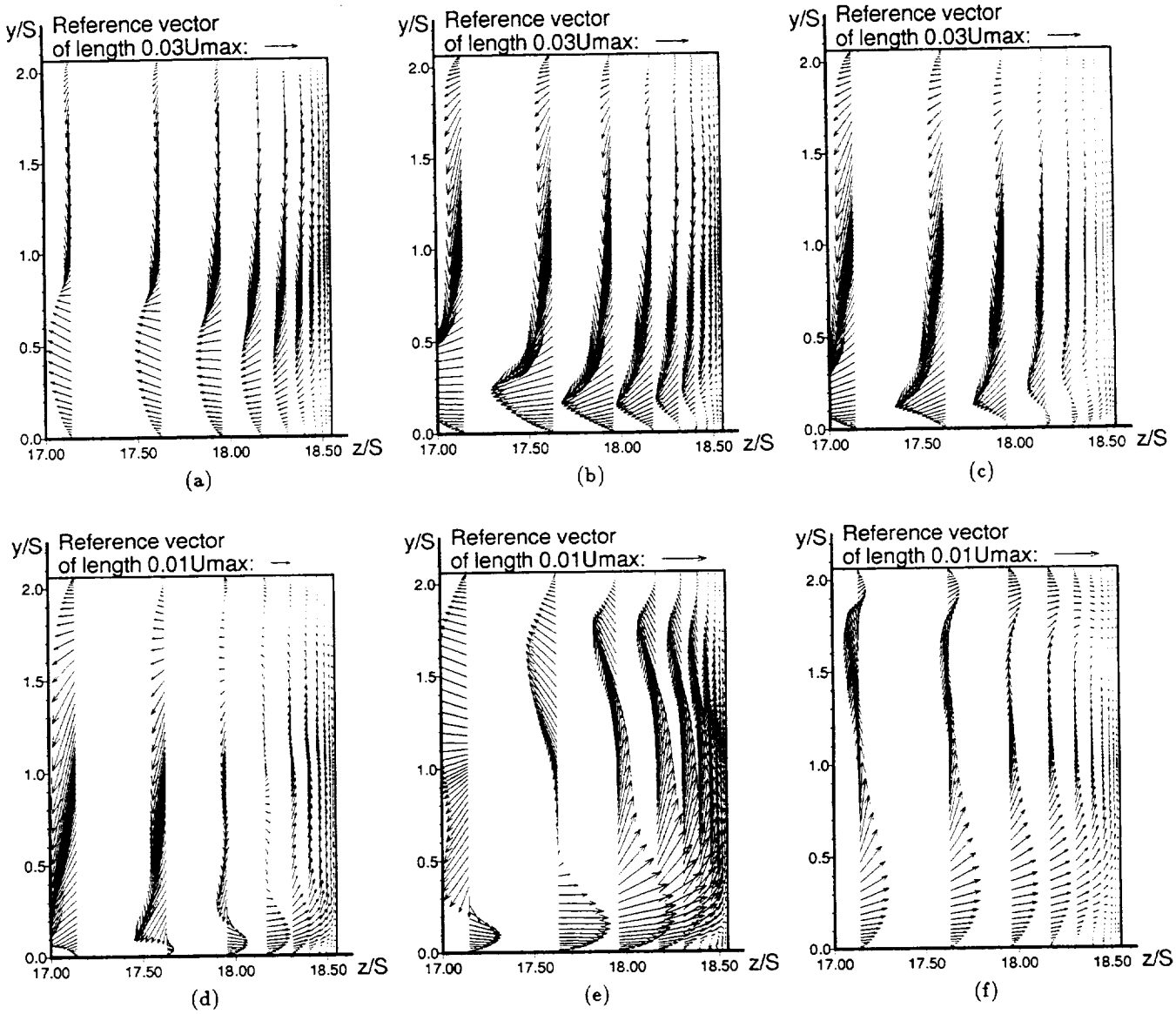

Figure 10. Cross-flow velocity vectors in constant-x cross-sections — $Re = 389$; three-dimensional simulation. (a) $x/S = 1.98$, (b) $x/S = 3.98$, (c) $x/S = 5.38$, (d) $x/S = 6.96$, (e) $x/S = 9.00$, (f) $x/S = 12.00$.

REFERENCES

Armaly, B. F., Durst, F., Pereira, J.C.F., and Schönung, B., 1983, "Experimental and Theoretical investigation of Backward-Facing Step Flow," *J. of Fluid Mechanics*, vol. 127, pp. 473–469.

Arnal, M., and Friedrich, R., 1991, "Investigation of the Pressure and Velocity Fields in a Turbulent Separated Flow Using the LES Technique," AIAA-91-0251.

Arnone, A., Liou, M.-S., and Povinelli, L. A., 1991, "Multigrid Calculation of Three-Dimensional Viscous Cascade Flows," AIAA-91-3238.

Arnone, A., Liou, M.-S., and Povinelli, L. A., 1992, "Navier-Stokes Solution of Transonic Cascade Flows Using Non-Periodic C-Type Grids," *Journal of Propulsion and Power*, vol. 8, pp. 410-417.

Coirier, W. J. and Van Leer, B., 1991, "Numerical Flux Formulas for the Euler and Navier-Stokes Equations, II. Progress in Flux-Vector Splitting," AIAA-41-1566. Also, NASA TM 104353.

Hasan, M. A. Z., 1992 "The Flow over a Backward-Facing Step Under a Controlled Separation: Laminar Separation," *J. of Fluid Mech.*, vol. 238, pp. 73–96.

Isomoto, K. and Honami, S., 1989, "The Effec of Inlet Turbulence Intensity on the Reattachment Process Over a Backward Facing Step," ASME *J. of Fluids Engineering*, vol. 111, pp. 87–92.

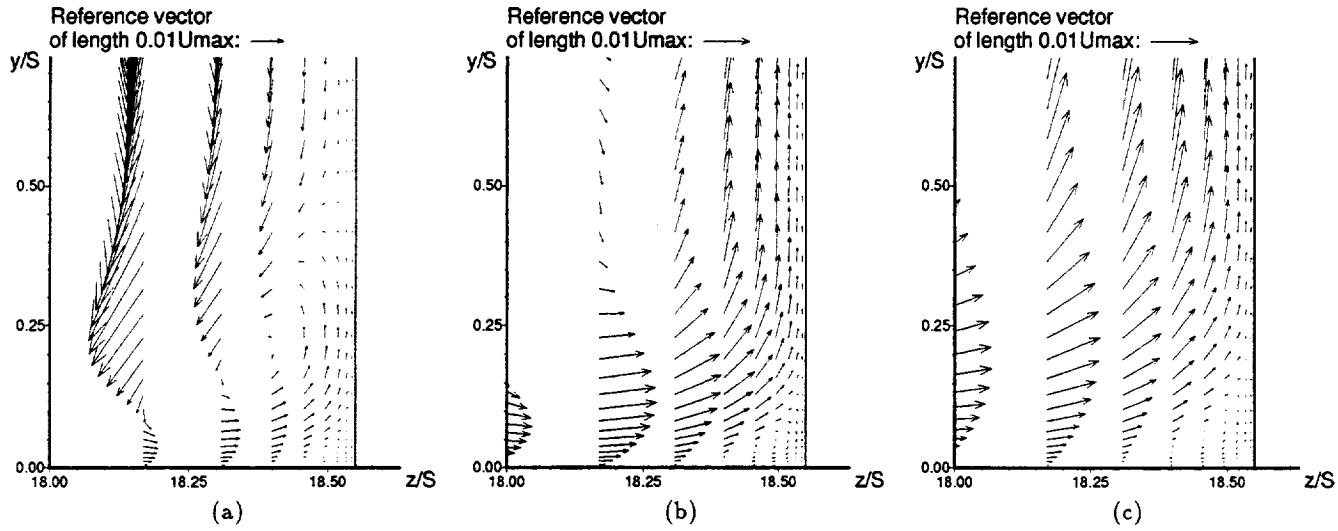

Figure 11. Cross-flow velocity vectors in constant-x cross-sections — $Re = 389$; three-dimensional simulation. Flow in corner between sidewall and channel floor: (a) $x/S = 5.38$, (b) $x/S = 6.96$, (c) $x/S = 9.00$.

Jameson, A., Schmidt, W., and Turkel, E., 1981, "Numerical Solutions of the Euler Equations by Finite Volume Methods Using Runge-Kutta Time-Stepping Schemes," AIAA-81-1259.

Kaiktsis, L., Karniadakis, G., E., and Orszag, S., A., 1991, "Onset of Three-dimensionality, Equilibria, and Early Transition in Flow over a Backward Facing Step," *J. of Fluid Mech.*, vol. 231, pp. 501-528.

Ku, H. C., Hirsh, R. S., Taylor, T. D., and Rosenberg, A. P., 1989, "A Pseudospectral Matrix Element Method for Solution of Three-Dimensional Incompressible Flows and its Parallel Implementation," *J. of Computational Physics*, vol. 83, pp. 260–290.

Liou, M.-S., and Steffen, C. J., 1991, "A New Flux Splitting Scheme," NASA TM 104404.

Schlichting, H., 1979, "Boundary-Layer Theory," McGraw-Hill, New York

Schmitt, L. and Friedrich, R., 1987, "Application of the Large-Eddy Simulation Technique to Turbulent Backward Facing Step Flow," Proceedings; Symposium on Turbulent Shear Flows, 6th, Toulouse, France, Sept. 7–9, 1987.

Silveira N., A., Grand, D., Metais, O., and Lesieur, M., 1991, "Large-Eddy Simulation of the Turbulent Flow in the Dowstream Reagion of a Backward Facing Step," *Physical Review Letters*, vol 66, no. 18, pp. 2320–2323.

Thangam, S. and Hur, N., 1991, "A Highly-Resolved Numerical Study of Turbulent Separated Flow Past a Backward-Facing Step," *Intern. J. of Eng. Science*, vol 29, no. 5, pp. 607-615.

Thangam, S. and Speziale, C. G., 1992, "Turbulent Flow Past a Backward-Facing Step: A Critical Evaluation of Two-Equation Models," AIAA *J.*, vol. 30, no. 5, pp. 1314–1320.

Tsou, F.K., Chen, S.-J., Aung, W., 1991, "Starting Flow and Heat Transfer Downstream of a Backward Facing Step," ASME *J. of Heat Transfer*, vol. 113, pp. 583–589.

Vogel, J. C. and Eaton, J. K., 1985, "Combined Heat Transfer and Fluid Dynamic Measurements Downstream of a Backward-Facing Step," ASME *J. of Heat Transfer*, vol. 107, pp. 922–929.

REPORT DOCUMENTATION PAGE

Form Approved
OMB No. 0704-0188

1. AGENCY USE ONLY (*Leave blank*)	2. REPORT DATE	3. REPORT TYPE AND DATES COVERED
	July 1993	Technical Memorandum

4. TITLE AND SUBTITLE

Numerical Simulations of Three-Dimensional Laminar Flow Over a Backward Facing Step; FLow Near Side Walls

5. FUNDING NUMBERS

WU-505-90-5K

6. AUTHOR(S)

Erlendur Steinthorsson, Meng-Sing Liou, Louis A. Povinelli, and Andrea Arnone

7. PERFORMING ORGANIZATION NAME(S) AND ADDRESS(ES)

National Aeronautics and Space Administration
Lewis Research Center
Cleveland, Ohio 44135-3191

8. PERFORMING ORGANIZATION REPORT NUMBER

E-7970

9. SPONSORING/MONITORING AGENCY NAME(S) AND ADDRESS(ES)

National Aeronautics and Space Administration
Washington, D.C. 20546-0001

10. SPONSORING/MONITORING AGENCY REPORT NUMBER

NASA TM-106248
ICOMP-93-21

11. SUPPLEMENTARY NOTES

Prepared for the 1993 ASME Fluids Engineering Division Summer Meeting Symposium on Separated Flows, sponsored by the American Society of Mechanical Engineers, Washington, D.C., June 20-24, 1993. Erlendur Steinthorsson and Andrea Arnone, Institute for Computational Mechanics in Propulsion, NASA Lewis Research Center (work funded under NASA Cooperative Agreement NCC3-233) and Meng-Sing Liou and Louis A. Povinelli, NASA Lewis Research Center. ICOMP Program Director, Louis A. Povinelli, (216) 433-5818.

12a. DISTRIBUTION/AVAILABILITY STATEMENT

Unclassified - Unlimited
Subject Category

12b. DISTRIBUTION CODE

13. ABSTRACT (*Maximum 200 words*)

This paper reports the results of numerical simulations of steady, laminar flow over a backward-facing step. The governing equations used in the simulations are the full "compressible" Navier-Stokes equations, solutions to which were computed by using a cell-centered, finite volume discretization. The convection terms of the governing equations were discretized by using the Advection Upwind Splitting Method (AUSM), whereas the diffusion terms were discretized using central differencing formulas. The validity and accuracy of the numerical solutions were verified by comparing the results to existing experimental data for flow at identical Reynolds numbers in the same backstep geometry. The paper focuses attention on the details of the flow field near the side wall of the geometry.

14. SUBJECT TERMS

Separated flows; Internal flow; Backward-facing step; Numerical simulations

15. NUMBER OF PAGES

10

16. PRICE CODE

A02

17. SECURITY CLASSIFICATION OF REPORT	18. SECURITY CLASSIFICATION OF THIS PAGE	19. SECURITY CLASSIFICATION OF ABSTRACT	20. LIMITATION OF ABSTRACT
Unclassified	Unclassified	Unclassified	